

Nodal phases in non-Hermitian wallpaper crystals

J. Lukas K. König,^{a)} Felix Herber,^{b)} and Emil J. Bergholtz^{c)}

Department of Physics, Stockholm University, AlbaNova University Center, 106 91 Stockholm, Sweden

(Dated: 30 October 2023)

Symmetry and non-Hermiticity play pivotal roles in photonic lattices. While symmetries such as parity-time (\mathcal{PT}) symmetry have attracted ample attention, more intricate crystalline symmetries have been neglected in comparison. Here, we investigate the impact of the 17 wallpaper space groups of two-dimensional crystals on non-Hermitian band structures. We show that the non-trivial space group representations enforce degeneracies at high symmetry points and dictate their dispersion away from these points. In combination with either \mathcal{T} or \mathcal{PT} , the symmorphic p4mm symmetry, as well as the non-symmorphic p2mg, p2gg, and p4gm symmetries, protect novel exceptional chains intersecting at the pertinent high symmetry points.

Introduction.

In the past decades, non-Hermitian effective descriptions have emerged as a central framework used to describe a wide variety of experimental setups¹. Generally, the non-Hermitian terms describe gain or dissipation in the respective systems. The applications can range from classical metamaterials through photonic crystals and quantum optics to open quantum systems.

The spectra of such systems differ significantly from their Hermitian counterparts². For one, non-Hermitian operators feature degenerate points with higher abundance; their codimension is two compared to three for Hermitian degeneracies^{3,4}. As such non-Hermitian degenerate points occur generically in two-dimensions. Furthermore, these degenerate points are deficient, so-called exceptional points (EPs), and feature non-differentiable dispersion relations³⁻⁷. In three dimensions they occur as exceptional lines that may form knots, links, and similar structures of topological interest⁸⁻¹³. Exceptional points occur readily in photonic systems, more so if a perfect balance of gain and loss renders these systems \mathcal{PT} -symmetric¹⁴⁻¹⁶.

In general, imposing symmetries^{17,18} on a given system increases the abundance and variety of stable nodal points. In non-Hermitian systems, symmetries such as \mathcal{PT} lead to EPs of codimension one, i.e. occurring generically in one dimension, forming stable lines in two dimensions and so on¹⁹⁻²⁷. Moreover, it increases the number of degenerate energy levels which may lead to the generic appearance of higher-order exceptional points²⁸⁻³⁴. Considering internal symmetries, the Hermitian Altland-Zirnbauer classification must be extended to a 38-fold symmetry classification for non-Hermitian systems^{35,36}. In Hermitian systems it is well-known that spatial symmetries can also enhance the abundance of nodal points, constrain them to particular shapes such as nodal chains³⁷, or enforce degenerate points at material surfaces³⁸, or at specific points of high symmetry³⁹.

Early results have extended these results to non-Hermitian systems, extending symmetry indicators⁴⁰, establishing the existence of crystalline-symmetry protected nodal chains in three-dimensional systems^{41,42}, studying \mathcal{PT} -symmetric optical lattices using the representation theory of colored groups⁴³ and the symmetry-protected degenerate points in two-dimensional square photonic lattices⁴⁴. Since exceptional points appear generically already in two dimensions, we expect a general characterization of two-dimensional symmetry-enforced features to be of interest.

Here we provide this characterization by listing all possible nodal structures that can be enforced by the thirteen symmorphic space groups in two dimensions. We find that seven of these groups feature points of high symmetry with non-trivial little group representations. These constrain the Hamiltonian to be degenerate at the points of high symmetry, featuring a Hermitian-type nodal point at which eigenvectors are orthogonal (in contrast to EPs where they are degenerate). Taking into account time reversal symmetry \mathcal{T} , or a combination of time reversal and spatial inversion symmetries \mathcal{PT} , novel and intrinsically non-Hermitian nodal structures emerge in the surrounding dispersion. In particular, the nodal points at the high-symmetry momenta of space group p4mm and p4gm (p2mg, p4gm, and p2gg) turn out to be the intersection of four (two) exceptional lines that are constrained to a particular point in momentum space. They resemble non-defective EPs, seen as limit points along these exceptional lines⁴⁵.

We begin our work by recapitulating the physical intuition of space groups, and how they give rise to and constrain the momentum-space Hamiltonian of crystalline systems. We continue by listing all space groups and momenta that give rise to non-trivial point group action, before explicitly enumerating the allowed Bloch Hamiltonians in the neighborhood of these points to lowest order. We then survey these same lowest-order terms for Bloch Hamiltonians constrained by spatial as well as either \mathcal{PT} or \mathcal{T} symmetry. Finally, we present simple lattice models that illustrate our main results.

Background. We investigate two-dimensional systems since non-Hermitian degeneracies, so-called exceptional

^{a)} lukas.konig@fysik.su.se

^{b)} fehe3416@student.su.se

^{c)} emil.bergholtz@fysik.su.se

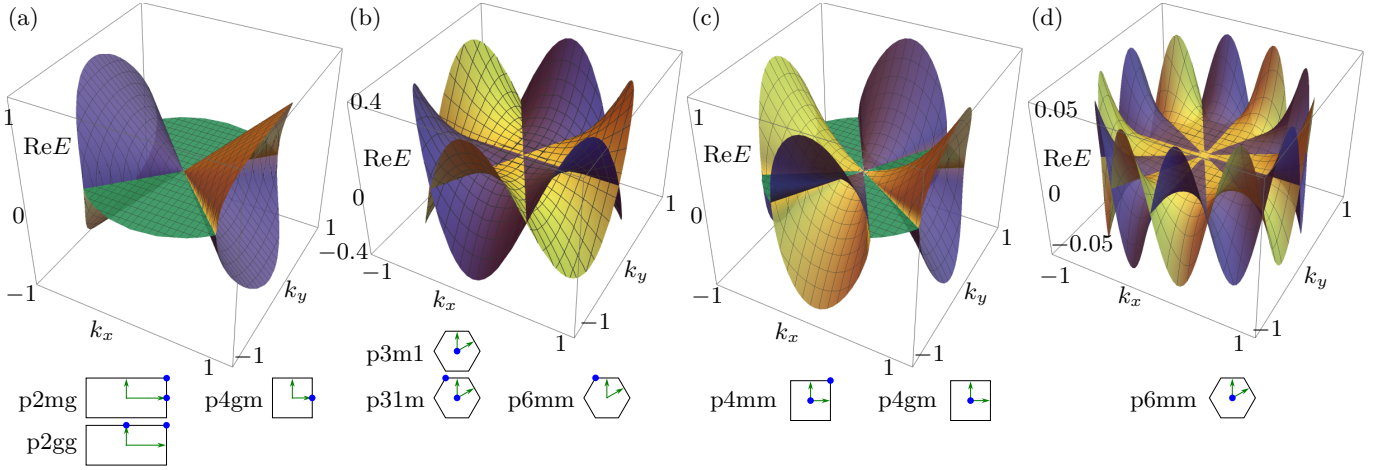


FIG. 1. Main result: For wallpaper groups p2mg, p2gg, p3m1, p31m, p4mm, p4gm, and p6mm, there exist points \mathbf{k}^* of high symmetry in the Brillouin zone that carry non-trivial point group representation. This enforces degenerate spectra at \mathbf{k}^* . For \mathcal{PT} -symmetric models it further enforces nodal lines emanating from \mathbf{k}^* . (a) Real part of typical low-energy dispersion relation around points with D_2 point group obtained from Eq. (12d) for $E_1 = E_2 = 1$. The two nodal lines consist of exceptional points. Inset are the Brillouin zones of the respective crystals, with corresponding points \mathbf{k}^* demarcated in blue. (b-d) as (a), for points with a D_3 (D_4 , D_6) point group; models given in Eqs. (13) with $A = \bar{B}_1 = \bar{B}_2 = C = 1$. Three nodal lines (four exceptional lines, six nodal lines) cross at \mathbf{k}^* .

points (EPs), occur generically with codimension two. We describe our process and results within the tight-binding approximation. States in the systems we consider are naturally expressed in a basis of orbitals, each of which is associated to a point $\mathbf{r} \in \mathbb{R}^2$ in the plane. In crystalline systems these are arranged periodically in a lattice, i.e., there are two linearly independent shortest lattice vectors $\mathbf{t}_1, \mathbf{t}_2 \in \mathbb{R}^2$ such that for each state at some \mathbf{r} there exists another state at $\mathbf{r} + n\mathbf{t}_1 + m\mathbf{t}_2$ for any $n, m \in \mathbb{Z}$. We thus label the periodic repetition by indices (n, m) , as well as another index j labeling the unit cell pattern that is repeated over the lattice. This means the Hilbert space is made up of states $|\phi_{n,m,j}\rangle$ that describe an orbital of the same type as $|\phi_{0,0,j}\rangle$, shifted by $n\mathbf{t}_1 + m\mathbf{t}_2$. The position associated to each basis state is then $\mathbf{r}(n, m, j) = n\mathbf{t}_1 + m\mathbf{t}_2 + \mathbf{r}_j$ for a fixed vector \mathbf{r}_j . We will equivalently denote the bases as $|\phi_j(\mathbf{r})\rangle$, suppressing the dependencies of \mathbf{r} .

Translations along the lattice vectors are represented on Hilbert space by operators $T_{\mathbf{t}_1}, T_{\mathbf{t}_2}$ which commute and act on the orbitals as a permutation,

$$T_{\mathbf{t}_1}^n T_{\mathbf{t}_2}^m |\phi_j(\mathbf{r})\rangle = |\phi_j(\mathbf{r} + n\mathbf{t}_1 + m\mathbf{t}_2)\rangle. \quad (1)$$

Depending on the given crystal, there exist further spatial transformations with simple action on the given position basis. Geometrically they correspond to isometries g on the Euclidean plane, and so are either rotations, reflections, or glide axes. Their unitary action on Hilbert space can be broken down into two parts: First, a state's position is changed by an operation $u_g : \mathbf{r}(n, m, j) \mapsto \mathbf{r}' = \mathbf{r}(n', m', l)$, and second, the different states within the same unit cell may be mixed by a non-trivial unitary U_g . This is for example the case for a reflection that ex-

changes a given orbital with its mirror image. The total action reads

$$\mathcal{U}_g |\phi_j(\mathbf{r}(n, m, j))\rangle = (U_g)_{jl} |\phi_l(\mathbf{r}(n', m', l))\rangle. \quad (2)$$

Together with the aforementioned translations, these isometries form the spatial symmetry group, or space group, of a given crystal. There are seventeen of these groups for two-dimensional systems, commonly referred to as *wallpaper groups*.

Momentum space. We will find it convenient to work in momentum space, i.e., transforming to a basis of Hilbert space in which the translation operators are diagonal. To make this mathematically coherent, we work in a lattice of finite size under periodic boundary conditions $\mathbf{r} \sim \mathbf{r} + N_a \mathbf{t}_1 \sim \mathbf{r} + N_b \mathbf{t}_2$ before performing the thermodynamic limit $N_a, N_b \rightarrow \infty$. The basis transformation takes the form

$$|\phi_j(\mathbf{k})\rangle = \frac{1}{\sqrt{N_a N_b}} \sum_{n,m} e^{-i\mathbf{k} \cdot \mathbf{r}(n,m,j)} |\phi_j(\mathbf{r}(n,m,j))\rangle, \quad (3)$$

a Fourier transform of the position basis. The dependence on crystalline momentum \mathbf{k} is periodic; alternatively \mathbf{k} can be thought of as defined up to addition of so-called reciprocal lattice vectors $\mathbf{g}_1, \mathbf{g}_2$. These satisfy $\mathbf{g}_i \cdot \mathbf{t}_j = 2\pi\delta_{ij}$ and are given, e.g., in Table III in Ref. 46. The momentum \mathbf{k} takes values in $(2\pi/N_a \mathbb{Z}, 2\pi/N_b \mathbb{Z})$, which turns continuous in the thermodynamic limit.

A translation acts diagonally on this state as $T_{\mathbf{t}_i} |\phi_l(\mathbf{k})\rangle = e^{i\mathbf{k} \cdot \mathbf{t}_i} |\phi_l(\mathbf{k})\rangle$ which can be seen by direct application of Eqs (1) and (3). Other spatial transformations act on spatial coordinates as $u_g : \mathbf{r} \mapsto \Delta_g \mathbf{r} + \delta_g$, where the point group part Δ_g is an orthogonal matrix

and δ_g is some shift that may be a fraction of a lattice vector. Such an operation acts on the momentum basis states as

$$U_g |\phi_j(\mathbf{k})\rangle = e^{i\Delta_g \mathbf{k} \cdot \delta_g} (U_g)_{jl} |\phi_l(\Delta_g \mathbf{k})\rangle \quad (4)$$

Symmetry. Physically, we describe a crystal by its Hamiltonian operator, for which the spatial transformations that leave the crystal invariant must constitute a symmetry. For the single-particle Hamiltonian with matrix elements

$$\langle \phi_{n',m',j'} | H | \phi_{n,m,j} \rangle = H_{j'j}(\mathbf{r}(n',m',j'), \mathbf{r}(n,m,j)), \quad (5)$$

translation invariance requires the position dependence to be $H_{j'j}(\mathbf{r}' - \mathbf{r})$. In this case, the Hamiltonian is block diagonal in the momentum basis: direct application of Eq. (3) gives $\langle \psi_{j'}(k') | H | \psi_j(k) \rangle = H_{j'j}(k) \delta(k - k')$ in the thermodynamic limit, where the so-called Bloch Hamiltonian has matrix elements

$$H_{j'j}(k) = \sum_{\substack{\rho = \mathbf{r}(n,m,j) - \mathbf{r}_{j'} \\ n,m}} e^{-2i\mathbf{k} \cdot \rho} H_{j'j}(\rho) \quad (6)$$

and constitutes the block diagonals of H . It depends continuously on \mathbf{k} .

Symmetry under non-translational spatial transformations that act according to Eq. (4) imply that the Bloch Hamiltonian is constrained further by

$$H(\mathbf{k}) = U_g H(\Delta_g \mathbf{k}) U_g^\dagger. \quad (7)$$

This means that the space group constraints carry over directly to Bloch Hamiltonians if Δ_g itself is a space group element, which is always the case for symmorphic space groups. For non-symmorphic groups, the occurring matrices U_g are not representations of the point group generated by elements Δ_g , and we treat these groups separately.

Altogether, the non-translation symmetries of a crystal further constrain the Hamiltonian describing it, effectively decreasing the unit cell by determining the Bloch Hamiltonian at points $H(\Delta \mathbf{k})$ given $H(\mathbf{k})$. Eq. (7) constitutes a particularly strong constraint at points of high symmetry \mathbf{k}^* that satisfy $\mathbf{k}^* = \Delta_g \mathbf{k}^*$ for some space group elements g . At these points,

$$H(\mathbf{k}^*) = U_g H(\mathbf{k}^*) U_g^\dagger, \quad (8)$$

and all group operations that keep \mathbf{k}^* invariant form its so-called little group. We investigate this constraint in the following.

Note that the unitary matrices appearing in Eq. (8) form a (projective) representation of the little group, as $U_{gh} = U_g U_h$. Such group representations decompose into irreducible representations, which means that there exists basis in which $H(\mathbf{k})$ is block diagonal and block-wise constrained by a simplest set of matrices $U_g^{(i)}$. We may thus focus on these blocks individually and assume

the constraining unitary matrices in Eq. (8) are irreducible representations of the little group. We focus here on these irreducible representations that have dimension greater than one and thus impose non-trivial constraints on $H(\mathbf{k})$. These irreducible representations correspond to physical relations between the orbitals in the unit cell, and constitute block diagonals of the matrix U_g in Eq. (4) for a conveniently chosen basis.

TABLE I. Wallpaper groups G (crystallographic notation) with high-symmetry momenta \mathbf{k}^* (in multiples of reciprocal lattice vectors) that can feature non-trivial representations of their respective little group $G^{\mathbf{k}^*}$ constraining Bloch Hamiltonian $H(\mathbf{k}^*)$. The final column denotes whether the momenta \mathbf{k}^* are invariant under time reversal \mathcal{T} . In p6mm a rotation about $2\pi/6$ maps the threefold rotation center at K to a different point that must thus carry the same representation. These are the K, K' points known from graphene. The corresponding space group representations are given in Eqs. (12).

G	\mathbf{k}^*	$G^{\mathbf{k}^*}$	\mathcal{T} -inv.
p3m1, p31m	$\Gamma = (0, 0)$	D_3	yes
p31m, p6mm*	$K = (-\frac{1}{3}, \frac{2}{3})$	D_3	no
p4mm, p4gm	$\Gamma = (0, 0)$	D_4	yes
p4mm	$M = (\frac{1}{2}, \frac{1}{2})$	D_4	yes
p6mm	$\Gamma = (0, 0)$	D_6	yes
p2mg	$S = (\frac{1}{2}, \frac{1}{2})$	D_2^*	yes
p2gg	$Y = (0, \frac{1}{2})$	D_2^*	yes
p2mg, p2gg, p4gm	$X = (\frac{1}{2}, 0)$	D_2^*	yes
p4gm	$M = (\frac{1}{2}, \frac{1}{2})$	D_4	yes

Results.

We list all points of high symmetry that carry a non-trivial representation of the respective wallpaper group in Table I. A complete list of such points including one-dimensional representations can be found in Ref. 46. We note that there exist additional non-trivial fermionic representations around the high-symmetry points of non-symmorphic wallpaper groups. In the context of photonics, we consider only bosonic representations, i.e., ones that map $|\phi(k)\rangle$ to itself with a phase of 2π under a full rotation.

We begin by discussing the symmorphic wallpaper groups, for which the only little groups carrying irreducible representations of dimension greater than one are the dihedral groups D_3, D_4 , and D_6 . Consequently only these can enforce degenerate $H(\mathbf{k}^*)$. We proceed to list the non-trivial representations following Ref. 47. The dihedral group D_n can be presented as

$$D_n = \langle r, m | r^n, m^2, mrmr \rangle, \quad (9)$$

i.e., it is generated by a rotation r of order n and a reflection m that satisfy $mr = r^{-1}m$. Their two-dimensional irreducible representations are generated by

$$\rho_h(r) = \text{diag}(\omega, \omega^{-1}) \quad \text{and} \quad \rho_h(m) = \sigma_x \quad (10)$$

where $\omega = e^{2\pi i h/n}$, σ_x is the standard Pauli matrix and $0 < h < \lceil \frac{n}{2} \rceil \in \mathbb{N}$ labels inequivalent representations.

It turns out that all these representations constrain $H(\mathbf{k}^*)$ in the same way, forcing it to be twofold degenerate: Applying Eq. (8) with U_g chosen to be the rotation and reflection generator imposes $H(\mathbf{k}^*) = d_0 I_2 + d_z \sigma_z$ and $H(\mathbf{k}^*) = d_0 I_2 + d_x \sigma_x$, respectively. In combination these constraints require $d_x = d_z = 0$. This means that a given crystalline symmetry forces the Bloch Hamiltonian to be degenerate, $E_1(\mathbf{k}^*) = E_2(\mathbf{k}^*) = d_0$. Non-Hermitian terms in the Hamiltonian do not change this result.

Note that it is impossible to open a gap at \mathbf{k}^* by adding terms that have appropriate D_n symmetry to individual bands, since it is the orbitals' spatial structure that determines which representation they transform under. The only remaining degree of freedom is $d_0 I_2$, which does not affect the gap structure.

Next we discuss the case of non-symmorphic space groups, whose representation theory is complicated slightly. These groups contain glide reflections, a combination of a reflection Δ_g and a subsequent shift along the reflection axis. The point group part of these transformations is the reflection Δ_g that is not itself a part of the wallpaper group. This reflection appears in Eq. (7), which means that while glide reflections have no fixed points in real space, the entire glide reflection axis constitutes fixed points in momentum space. Correspondingly, intersections of such axes are points of higher symmetry. The irreducible representations in terms of U_g for the relevant groups at these points come in two distinct classes and are listed explicitly in Ref. 46.

One class of representations occurs at points where two reflection axes intersect. It is given by

$$\rho^*(r) = \sigma_x, \quad \text{and} \quad \rho^*(g_x) = \sigma_y \quad (11)$$

where r is the rotation about π and g_x is the glide reflection along the x -axis. This is a representation of a non-Abelian double cover of D_2 in which one of the reflection transformations squares to -1 , so we denote this as D_2^* . The second class occurs at the center of the Brillouin zone of $p4gm$, where two reflection axes and two glide reflection axes intersect. The representation is equivalent to the one of D_4 , except for a factor of -1 as for the case of D_2^* , which is irrelevant in Eq. (7). As for the symmorphic groups, all of these representations enforce degenerate $H(\mathbf{k}^*)$.

Dispersion. We investigate next how non-Hermitian terms affect the dispersion relation around the degenerate points of high symmetry. Without loss of generality, we consider traceless operators, setting $d_0 = 0$. Note that the omitted trace terms must also be symmetric under the space group action. In particular, tilting of the occurring dispersion is generally disallowed.

In a neighborhood $\mathbf{k} \approx \mathbf{k}^*$ we consider the symmetry constraint (7) order by order in the Taylor expansion of

the Bloch Hamiltonian. Direct calculation gives

$$H^{(D_3)}(\mathbf{k}) = A(k_x \sigma_x + k_y \sigma_y) + \mathcal{O}(\mathbf{k}^2) \quad (12a)$$

$$H^{(D_4)}(\mathbf{k}) = B_1(k_x^2 - k_y^2)\sigma_x + iB_2k_xk_y\sigma_y + \mathcal{O}(\mathbf{k}^4) \quad (12b)$$

$$H^{(D_6)}(\mathbf{k}) = C[(k_x^2 - k_y^2)\sigma_x \mp 2k_xk_y\sigma_y] + \mathcal{O}(\mathbf{k}^4) \quad (12c)$$

$$H^{(D_2^*)}(\mathbf{k}) = iE_1k_y\sigma_y + E_2k_x\sigma_z + \mathcal{O}(\mathbf{k}^2). \quad (12d)$$

up to unitary, where we chose the coordinate system s.t. the x -axis constitutes a reflection axis. The two signs correspond to the $h = 1, 2$ representations of D_6 and we introduce arbitrary constants $A, B_1, B_2, C, E_1, E_2 \in \mathbb{C}$. The dispersion imposed by D_3 -symmetry is precisely the low-energy excitation Hamiltonian of graphene at the K point. Notably, under both D_4 and D_6 contributions at first order in \mathbf{k} are forbidden, imposing a \mathbf{k}^2 -dispersion on the low-energy excitations. For D_4 and D_2^* symmetries there is a second complex degree of freedom, allowing for a range of possible spectra.

Additional symmetries. Given that both spatial and non-spatial symmetries are known to constrain spectra significantly, it is quite natural to investigate their interplay.

To start with, we note that imposing Hermitian “symmetry”, $H = H^\dagger$, only imposes real multiplicative prefactors in Eq.s (12). This does not qualitatively alter the low-energy excitation Hamiltonians constrained by D_3 and D_6 , while for D_4 and D_2^* it imposes $B_1, iB_2, iE_1, E_2 \in \mathbb{R}$ and thus constrains the systems qualitatively.

We next investigate the effects of \mathcal{PT} symmetry, which is of particular experimental relevance in non-Hermitian systems. It corresponds to, e.g., balanced gain and loss in optical setups and is realized among others in photonic crystals. As a symmetry constraint it reduces the codimension of nodal structures further, leading to the generic appearance of nodal lines in the two dimensional systems considered here²⁶. In its most straightforward representation, it requires the Bloch Hamiltonian to be real at each \mathbf{k} . For two-band Hamiltonians, this only allows for terms $\sigma_x, i\sigma_y, \sigma_z$ with real prefactors each, which fundamentally alters the results given in Eq.s (12). For the four groups of relevance, the allowed terms at lowest order are

$$H^{(D_3, \mathcal{PT})}(\mathbf{k}) = A\left(k_x^2k_y - \frac{1}{3}k_y^3\right)\sigma_z + \mathcal{O}(\mathbf{k}^5), \quad (13a)$$

$$H^{(D_4, \mathcal{PT})}(\mathbf{k}) = B_1(k_x^2 - k_y^2)\sigma_x + iB_2k_xk_y\sigma_y + \mathcal{O}(\mathbf{k}^4), \quad (13b)$$

$$H^{(D_6, \mathcal{PT})}(\mathbf{k}) = C\left(k_x^3k_y^3 - \frac{3}{10}(k_xk_y^5 + k_yk_x^5)\right)\sigma_z + \mathcal{O}(\mathbf{k}^8), \quad (13c)$$

$$H^{(D_2^*, \mathcal{PT})}(\mathbf{k}) = iE_1k_y\sigma_y + E_2k_x\sigma_z + \mathcal{O}(\mathbf{k}^2). \quad (13d)$$

with real constants A, B_1, B_2, C, E_1, E_2 , illustrated in Fig. 1. Here the first-order contribution we found for the

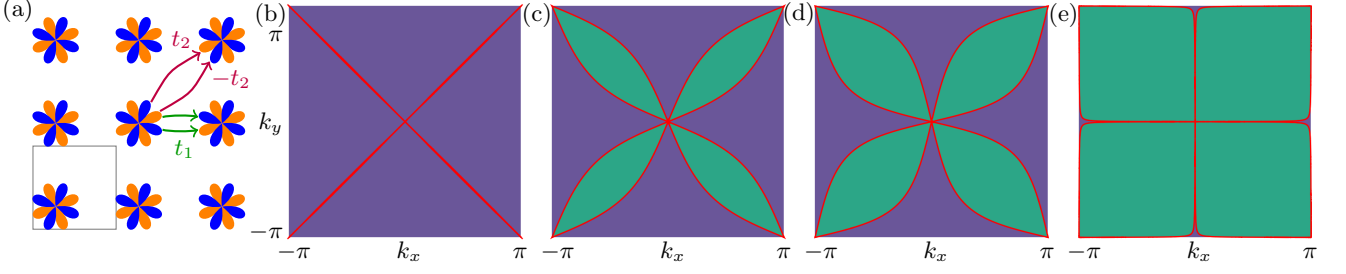


FIG. 2. (a) Lattice model corresponding to Eq. (14). In a square lattice, two orbitals (blue, orange) are located at the same position in a unit cell. They are fourfold rotation symmetric and each other's mirror image. Under reversal of drawn hoppings in horizontal and vertical directions are symmetric, while diagonal t_2 -hopping terms obtain a minus sign. All hoppings gain an additional minus sign for each rotation about $\pi/2$ relative to the hoppings shown in the figure. Under \mathcal{PT} symmetry, both t_1 and t_2 are real; t_2 constitutes anti-Hermitian NNN hopping. (b-e) Eigenvalue gap ΔE^2 shown for parameters $t_1/t_2 = 100$ (2, 1, 0.01) over the entire Brillouin zone. Green (blue) indicates regions with imaginary (real) eigenvalues. These regions are bounded by exceptional lines drawn in red.

case of D_3 is forbidden by \mathcal{PT} -symmetry, and the first non-trivial \mathcal{PT} -symmetric contribution occurs instead at third order. Under the combination of D_4 and \mathcal{PT} symmetry, the non-trivial term we found in Eq. (12b) is allowed, for a specific choice of coefficients. This constrains the model to an interesting corner of parameter space, since the spectrum in this case necessarily features four exceptional lines that emanate from the nodal point at \mathbf{k}^* . These lie at angle $2\theta = \pm \arctan(2(B_1/B_2)^2)$ relative to the coordinate axes. Finally, for dispersion around a point constrained by D_6 , the first allowed \mathcal{PT} -symmetric term occurs at sixth order for either representation.

Finally we note that time reversal \mathcal{T} acts similarly to \mathcal{PT} symmetry. In its simplest representation it also conjugates the Bloch Hamiltonian, with the added complication that it also inverts momentum $\mathbf{k} \mapsto -\mathbf{k}$. Models with point groups that contain a half turn are \mathcal{P} -invariant, and hence the two symmetries are equivalent. In fact, we find that for fixed points under inversion the two constraints are equivalent for all representations discussed. We expect a further interesting constraint for the K -point in $p6mm$, which is mapped to K' by both \mathcal{T} and a rotation about $2\pi/6$; the specifics depend on the given representation of the rotation. We conclude by noting that this means \mathcal{T} -invariance also leads to lines of EPs crossing at $\mathbf{k} = \mathbf{k}^*$ for D_4 and D_2 symmetries, as shown for \mathcal{PT} in Fig. 1.

Lattice models. We realize the allowed first-order terms Eqs. (12b) and (12d) in the overall D_4 -symmetric, respectively D_2^* -symmetric models

$$H_4(\mathbf{k}) = 2t_1[\cos(k_x) - \cos(k_y)] \sigma_x \quad (14)$$

$$+ 2it_2[\cos(k_x - k_y) - \cos(k_x + k_y)] \sigma_y$$

$$H_2(\mathbf{k}) = 2e_1 \sin(k_y) \sigma_y + 2e_2 \sin(k_x) \sigma_z \quad (15)$$

where we neglected the traceful parts $d_0(\mathbf{k})I_2$ as we are mainly interested in the gap structure.

We show the spectrum of H_4 in Fig. 2, and recover $B_1 = t_1$ and $B_2 = 4t_2$ in the low-energy expansion around the D_4 -symmetry point. Note that the only other

allowed nearest-neighbor hopping terms contribute proportional to σ_0 and do not affect the gap structure, since terms within the same sublattice of the form $f(\mathbf{k})\sigma_z$ must satisfy $f(k_x, k_y) = -f(-k_x, k_y) = -f(k_y, k_x)$ and thus vanish on the reflection axes.

Under \mathcal{PT} symmetry, both models show exceptional lines spanning the Brillouin zone, which intersect precisely at the high-symmetry points.

Conclusion.

In this work we surveyed the possible nodal structures constrained by the two-dimensional wallpaper groups. We found seven space groups with high-symmetry momenta at which the crystalline symmetry alone enforces nodal points. The surrounding dispersion is particularly interesting in distinction to known Hermitian results when, on top of its crystalline structure, the system is \mathcal{T} or \mathcal{PT} -symmetric. As our results are derived from symmetry considerations, we expect them to be valid also outside of the tight-binding approximation and relevant to experimental systems in several realms of physics, notably two-dimensional photonic crystal lattices.

We expect a full treatment of extended symmetry groups, using the representation theory of magnetic space groups, to produce a multitude of new and non-Hermitian nodal structure, as the extended symmetry may mix different irreducible representations of the space group. Another exciting prospect of this consideration is the emergence of higher order degeneracy. A hint that this can be fruitful is that \mathcal{PT} -symmetry alone makes third order EPs generic and stable in two dimensions^{28,29}.

An even more ambitious outlook is to extend the analysis given here to three dimensions. This is a major task given that there are 230 space groups in three-dimensions, and that three-dimensional non-Hermitian systems generically feature exceptional lines even in absence of symmetry. Completing such a program would amount to a photonics counterpart to the paradigm of topological quantum chemistry⁴⁸.

ACKNOWLEDGMENTS

JLKK and EJB were supported by the Swedish Research Council (VR, grant 2018-00313), the Wallenberg Academy Fellows program (2018.0460) and the project Dynamic Quantum Matter (2019.0068) of the Knut and Alice Wallenberg Foundation, as well as the Göran Gustafsson Foundation for Research in Natural Sciences and Medicine.

- ¹Y. Ashida, Z. Gong, and M. Ueda, *Advances in Physics* **69**, 249 (2020).
- ²E. J. Bergholtz, J. C. Budich, and F. K. Kunst, *Reviews of Modern Physics* **93**, 015005 (2021).
- ³M. Berry, *Czechoslovak Journal of Physics* **54**, 1039 (2004).
- ⁴W. D. Heiss, *Journal of Physics A: Mathematical and Theoretical* **45**, 444016 (2012), arxiv:1210.7536.
- ⁵T. Katō, *Perturbation Theory for Linear Operators*, Classics in Mathematics (Springer, Berlin, 1995).
- ⁶H. Zhou, C. Peng, Y. Yoon, C. W. Hsu, K. A. Nelson, L. Fu, J. D. Joannopoulos, M. Soljačić, and B. Zhen, *Science* **359**, 1009 (2018).
- ⁷V. Kozii and L. Fu, *Non-Hermitian Topological Theory of Finite-Lifetime Quasiparticles: Prediction of Bulk Fermi Arc Due to Exceptional Point* (2017), arxiv:1708.05841 [cond-mat].
- ⁸J. Carlström and E. J. Bergholtz, *Physical Review A* **98**, 042114 (2018).
- ⁹J. Carlström, M. Stålhammar, J. C. Budich, and E. J. Bergholtz, *Physical Review B* **99**, 161115 (2019).
- ¹⁰A. Cerjan, S. Huang, M. Wang, K. P. Chen, Y. Chong, and M. C. Rechtsman, *Nature Photonics* **13**, 623 (2019).
- ¹¹Y. Xu, S.-T. Wang, and L.-M. Duan, *Physical Review Letters* **118**, 045701 (2017).
- ¹²Z. Yang, C.-K. Chiu, C. Fang, and J. Hu, *Physical Review Letters* **124**, 186402 (2020).
- ¹³X. Zhang, G. Li, Y. Liu, T. Tai, R. Thomale, and C. H. Lee, *Communications Physics* **4**, 1 (2021).
- ¹⁴M.-A. Miri and A. Alù, *Science* **363**, eaar7709 (2019).
- ¹⁵A. Regensburger, C. Bersch, M.-A. Miri, G. Onishchukov, D. N. Christodoulides, and U. Peschel, *Nature* **488**, 167 (2012).
- ¹⁶Y. Zhang, S. Xia, L. Qin, Q. Wang, P. Jia, W. Qi, X. Feng, Y. Jiang, Z. Zhu, X. Zhao, W. Liu, and Y. Liu, *Applied Physics Letters* **123**, 161107 (2023).
- ¹⁷C.-K. Chiu, J. C. Y. Teo, A. P. Schnyder, and S. Ryu, *Reviews of Modern Physics* **88**, 035005 (2016).
- ¹⁸W. B. Rui, Z. Zheng, C. Wang, and Z. D. Wang, *Physical Review Letters* **128**, 226401 (2022).
- ¹⁹J. C. Budich, J. Carlström, F. K. Kunst, and E. J. Bergholtz, *Physical Review B* **99**, 041406 (2019).
- ²⁰K. Kawabata, T. Bessho, and M. Sato, *Physical Review Letters* **123**, 066405 (2019).
- ²¹K. Kimura, T. Yoshida, and N. Kawakami, *Physical Review B* **100**, 115124 (2019).
- ²²R. Okugawa and T. Yokoyama, *Physical Review B* **99**, 041202 (2019).
- ²³A. Szameit, M. C. Rechtsman, O. Bahat-Treidel, and M. Segev, *Physical Review A* **84**, 021806 (2011).
- ²⁴T. Yoshida, R. Peters, N. Kawakami, and Y. Hatsugai, *Physical Review B* **99**, 121101 (2019).
- ²⁵H. Zhou, J. Y. Lee, S. Liu, and B. Zhen, *Optica* **6**, 190 (2019).
- ²⁶K. Yang, Z. Li, J. L. K. König, L. Rødland, M. Stålhammar, and E. J. Bergholtz, *Homotopy, Symmetry, and Non-Hermitian Band Topology* (2023), arxiv:2309.14416 [cond-mat, physics:math-ph, physics:physics, physics:quant-ph].
- ²⁷K. Ding, C. Fang, and G. Ma, *Nature Reviews Physics* **4**, 745 (2022).
- ²⁸I. Mandal and E. J. Bergholtz, *Physical Review Letters* **127**, 186601 (2021).
- ²⁹P. Delplace, T. Yoshida, and Y. Hatsugai, *Physical Review Letters* **127**, 186602 (2021).
- ³⁰S. Sayyad and F. K. Kunst, *Physical Review Research* **4**, 023130 (2022).
- ³¹M. Stålhammar and E. J. Bergholtz, *Physical Review B* **104**, L201104 (2021).
- ³²J. Hu, R.-Y. Zhang, Y. Wang, X. Ouyang, Y. Zhu, H. Jia, and C. T. Chan, *Nature Physics* , 1 (2023).
- ³³L. Crippa, J. C. Budich, and G. Sangiovanni, *Physical Review B* **104**, L121109 (2021).
- ³⁴K. Wang, L. Xiao, H. Lin, W. Yi, E. J. Bergholtz, and P. Xue, *Science Advances* **9**, eadi0732 (2023).
- ³⁵K. Kawabata, K. Shiozaki, M. Ueda, and M. Sato, *Physical Review X* **9**, 041015 (2019).
- ³⁶H. Zhou and J. Y. Lee, *Physical Review B* **99**, 235112 (2019).
- ³⁷T. Bzdušek, Q. Wu, A. Rüegg, M. Sigrist, and A. A. Soluyanov, *Nature* **538**, 75 (2016).
- ³⁸B. J. Wieder, B. Bradlyn, Z. Wang, J. Cano, Y. Kim, H.-S. D. Kim, A. M. Rappe, C. L. Kane, and B. A. Bernevig, *Science* **361**, 246 (2018).
- ³⁹B. Bradlyn, J. Cano, Z. Wang, M. G. Vergniory, C. Felser, R. J. Cava, and B. A. Bernevig, *Science* **353**, aaf5037 (2016).
- ⁴⁰K. Shiozaki and S. Ono, *Physical Review B* **104**, 035424 (2021).
- ⁴¹R.-Y. Zhang, X. Cui, W.-J. Chen, Z.-Q. Zhang, and C. T. Chan, *Communications Physics* **6**, 1 (2023).
- ⁴²X. Cui, R.-Y. Zhang, X. Wang, W. Wang, G. Ma, and C. T. Chan, *Experimental realization of stable exceptional chains protected by non-Hermitian latent symmetries unique to mechanical systems* (2023), arxiv:2304.10347 [physics, physics:quant-ph].
- ⁴³A. Mock, *Optics Express* **24**, 22693 (2016).
- ⁴⁴A. Mock, *Physical Review A* **95**, 043803 (2017).
- ⁴⁵S. Sayyad, M. Stålhammar, L. Rodland, and F. K. Kunst, *Symmetry-protected exceptional and nodal points in non-Hermitian systems* (2022), arxiv:2204.13945 [cond-mat, physics:quant-ph].
- ⁴⁶A. P. Cracknell, *Thin Solid Films* **21**, 107 (1974).
- ⁴⁷C. J. Bradley and A. P. Cracknell, *The Mathematical Theory of Symmetry in Solids: Representation Theory for Point Groups and Space Groups*, Oxford Classic Texts in the Physical Sciences (Clarendon Press, Oxford, 2010).
- ⁴⁸B. Bradlyn, L. Elcoro, J. Cano, M. G. Vergniory, Z. Wang, C. Felser, M. I. Aroyo, and B. A. Bernevig, *Nature* **547**, 298 (2017).